

# Off-resonance Blurring Tolerant Image Reconstruction of 3D Radial MRI with Linogram Sampling

Naoharu Kobayashi<sup>1</sup>, Djaudat Idiyatullin<sup>1</sup>, Curtis A Corum<sup>1</sup>, and Michael Garwood<sup>1</sup>

<sup>1</sup>Center for Magnetic Resonance Research, Department of Radiology, University of Minnesota, Minneapolis, MN, United States

## Introduction

While off-resonance effects due to magnetic susceptibility differences and chemical shifts generate image distortion and/or displacement in Cartesian MRI, they result in blurring in reconstructed images in radial MRI, which is one major disadvantage of using radial MRI. Linogram sampling is a “semi-Cartesian” k-space sampling in radial MRI, where the sampling pattern is a concentric cube grid for 3D k-space sampling<sup>1,2</sup> (Fig.1a). In linogram sampling, points on each concentric cube plane are rectilinear and equispaced like a conventional Cartesian grid. Moreover, linogram sampling has one preferable off-resonance property that when the cubic k-space is divided to six pyramidal regions, each pyramid has a common time axis that is perpendicular to the cubic plane, namely, all points on each concentric cube plane accumulate the same off-resonance phase. This property is similar to the conventional Cartesian MRI that has a common time axis (the readout direction) in the entire k-space region. Here, we introduce a 3D radial MRI method tolerant to off-resonance blurring by combining the linogram k-space sampling, Hermitian extrapolation and a 3D ultra-short echo time sequence known as SWIft Imaging with Fourier Transformation (SWIFT)<sup>3</sup>.

## Method

SWIFT achieves nearly zero echo time (TE = a few microseconds) by quasi-simultaneous excitation and acquisition with a gapped frequency-modulated pulse. Therefore, the center of the k-space is free from off-resonance phase; thereby, the k-space shows nearly perfect Hermitian symmetry about the k-space center. Using the symmetry, a half of the k-space region can be extrapolated from the other half. By extrapolating a pyramid region in the linogram k-space, a pair of pyramids facing each other can be recovered. Since the facing pyramids have a common time axis perpendicular to the cubic plane, the off-resonance artifacts appear as distortion or displacement in image domain in a similar way to Cartesian MRI. Spherical sampling also has Hermitian symmetry, but it cannot have a common time axis, because the points with the same off-resonance phase sit on a spherical curved plane (Fig.1b). Therefore, the proposed processing works only for linogram datasets.

Image reconstruction of linogram datasets was performed in the following steps: (1) pick up 3 orthogonal pyramid regions, (2) calculate missing 3 pyramids according to Hermitian symmetry, (3) calculate the Fourier transform (FT) of the 2D square k-space in each rectilinear and equispaced cubic plane with chirp-Z transform<sup>4,5</sup>, and (4) apply 1D FT along the dimension perpendicular to the 2D chirp-Z transform planes.

The proposed reconstruction method was tested by numerical Bloch simulation. A SWIFT simulation dataset with linogram sampling was generated under the following condition: bandwidth = 125 kHz, gapped stretched hyperbolic secant (HS2) pulse excitation, matrix size = 320<sup>3</sup> (390 Hz/pixel), and total number of views = 117,600 (for all 6 pyramids). A 3D theoretical phantom with spin density and off-resonance distributions in space (Fig.2a) was used for the simulation. For comparison, simulation with spherical sampling was performed with the same sequence parameters except for the sampling pattern.

*In vivo* human dental imaging was carried out for experimental validation of the proposed method. MR scans were performed with a 4T horizontal scanner (Agilent Technologies, Inc.). Sequence parameters for SWIFT scans were as follow: bandwidth = 62.5 kHz, gapped HS2 pulse excitation, flip angle = 4°, TR = 4.4 ms, matrix size = 256<sup>3</sup> (244 Hz/pixel), total number of views = 75,264 and 65,536 for linogram and spherical k-space sampling, respectively. To show tolerance to off-resonance, images were reconstructed with a frequency offset of 250 Hz relative to the resonance frequency.

## Results and Discussion

In simulation, the image reconstructed with all 6 pyramid k-space regions shows blurry stripe patterns and edges, which is similar to the image from the spherical sampling dataset (Fig.2b). When all 6 pyramids are used for reconstruction, the two facing pyramids have different time axes, each of which points in the opposite direction to the other, resulting in inconsistent image distortion between the two pyramids (i.e., blurring). When 3 pyramids were used and the other 3 were extrapolated using Hermitian symmetry, the blur due to off-resonance was cleaned up and off-resonance artifacts became mostly distortion (Fig.2c). Depending on choice of the 3 pyramids used for reconstruction, the reconstructed image showed different distortion patterns. Furthermore, the 3 pyramids have mutually orthogonal time axes; thereby, there were “diagonal line” artifacts observed for some combinations (yellow arrow heads in Fig.2c). In human dental imaging, similar improvements were seen (Fig.3). The proposed reconstruction removed the blur around the boundaries between the teeth and soft tissues.

## Conclusion

SWIFT acquisition with linogram sampling and Hermitian extrapolation in reconstruction removed off-resonance blurring that is common in radial MRI sequences; the off-resonance artifacts became displacement/distortion of images, which is similar to Cartesian MRI.

## Acknowledgements

This research is supported by National Institutes of Health grant P41 EB015894, S10 RR023730 and S10 RR027290 and WM KECK Foundation.

## References

- (1) Axel L, et.al., *IEEE Trans. Med. Imaging* 1990;9:447-449, 1990.
- (2) Herman GT, et.al., *Phys. Med. Biol.* 37:673-687, 1992.
- (3) Idiyatullin D, et.al., *JMR* 181:342-349, 2006.
- (4) Rabiner LR., et.al., *IEEE Trans. Audio Electroacoust.* AU-17:86-92, 1969.
- (5) Kobayashi N, et.al., *Proc. ISMRM* 20:4256, 2012.

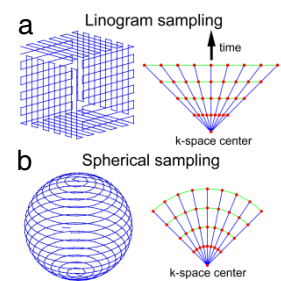


Fig.1. Linogram sampling (a) and Spherical sampling (b). Data points with the same off-resonance phase sit on straight planes (green lines) for linogram sampling and on spherical curved planes for spherical sampling.

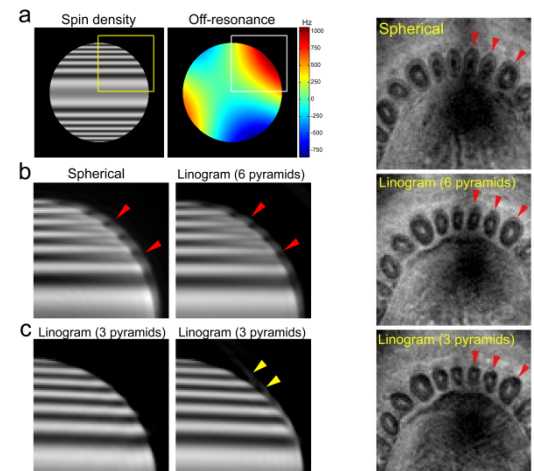


Fig.2. A numerical phantom in simulation (a) and reconstructed images from full datasets with spherical and linogram sampling (b). (c) Reconstructed images from the proposed reconstruction with different combinations of 3 pyramid regions (left and right).

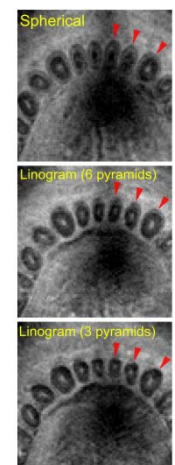


Fig.3. *In vivo* human tooth images from datasets with spherical and linogram sampling. The proposed reconstruction removed the blurry edges between tooth and soft tissues (red arrow heads).